Identification of prostamides, fatty acyl ethanolamines, and their biosynthetic precursors in rabbit cornea[S]

Paula Urquhart,* Jenny Wang,† David F. Woodward,† and Anna Nicolaou[1,*]

Manchester Pharmacy School,* The University of Manchester, Faculty of Medical and Human Sciences, Manchester, UK; and Department of Biological Sciences,† Allergan Inc., Irvine, CA

Abstract **Arachidonoyl ethanolamine (anandamide) and prostaglandin ethanolamines (prostamides) are biologically active derivatives of arachidonic acid. Although available through different precursor phospholipids, there is considerable overlap between the biosynthetic pathways of arachidonic acid-derived eicosanoids and anandamide-derived prostamides. Prostamides exhibit physiological actions and are involved in ocular hypotension, smooth muscle contraction, and inflammatory pain. Although topical application of bimatoprost, a structural analog of prostaglandin $F_{2\alpha}$ ethanolamide ($PGF_{2\alpha}$-EA), is currently a first-line treatment for ocular hypertension, the endogenous production of prostamides and their biochemical precursors in corneal tissue has not yet been reported. In this study, we report the presence of anandamide, palmitoyl-, stearoyl-, α-linolenoyl docosahexaenoyl-, linoleoyl-, and oleoyl-ethanolamines in rabbit cornea, and following treatment with anandamide, the formation of $PGF_{2\alpha}$-EA, PGE_2-EA, PGD_2-EA by corneal extracts (all analyzed by LC/ESI-MS/MS). A number of *N*-acyl phosphatidylethanolamines, precursors of anandamide and other fatty acyl ethanolamines, were also identified in corneal lipid extracts using ESI-MS/MS. These findings suggest that the prostamide and fatty acid ethanolamine pathways are operational in the cornea and may provide valuable insight into corneal physiology and their potential influence on adjacent tissues and the aqueous humor.**—Urquhart, P., J. Wang, D. F. Woodward, and A. Nicolaou. **Identification of prostamides, fatty acyl ethanolamines, and their biosynthetic precursors in rabbit cornea.** ***J. Lipid Res.*** **2015.** 56: **1419–1433.**

Supplementary key words anandamide • prostaglandin ethanolamine • *N*-acyl phosphatidylethanolamine • prostaglandin • cyclooxygenase • prostaglandin synthase • fatty acid amide hydrolase • *N*-acyl phosphatidylethanolamine phospholipase D • liquid chromatography tandem mass spectrometry • ocular tissue

The cornea functions to refract light and protect the intraocular structures of the eye. While its outermost epithelial layer facilitates oxygen diffusion and acts to absorb UV radiation (UVR), the innermost endothelial layer contributes to corneal transparency that is essential for optimum vision and regulates ocular pressure (1). Although a healthy cornea is avascular of blood and lymph vessels, hypertension or glaucoma can cause injury through abrasion of the endothelial cell lining leading to neovascularization, which if uncontrolled causes scarring and can lead to blindness (2, 3). Prostanoids are important regulators of corneal homeostasis with prostaglandin (PG) E_2 and thromboxane (TX) A_2 mediating corneal endothelial cell proliferation (4–6). While PGE_2 is also involved in angiogenesis and polymorphonuclear monocyte recruitment (7), PGD_2 can suppress corneal tumor growth and hyperpermeability (8). Furthermore, analogs of PGs are used as ocular hypotensive agents with bimatoprost, a structural analog of $PGF_{2\alpha}$ ethanolamide ($PGF_{2\alpha}$-EA), being widely used to treat glaucoma (9).

Prostaglandin ethanolamines (prostamides; PG-EAs) are sequentially biosynthesized from the endocannabinoid arachidonoyl ethanolamine (anandamide; A-EA) by cyclooxygenase (COX)-2 followed by various prostaglandin synthases (PGSs) (10–13). Anandamide is released from precursor phospholipids *N*-arachidonoyl phosphatidylethanolamines (NArPE) via *N*-acyl phosphatidylethanolamine (NAPE)-specific phospholipase (PL) D (NAPE-PLD), although recent findings have indicated the existence of other pathways mediated by either α,β-hydrolase 4 followed by cleavage of glycerophosphate to yield A-EA, or PLC and subsequent dephosphorylation of phosphoanandamide to A-EA [reviewed in (14)]. The majority of studies investigating these

This work was supported by Allergan Inc. through a research grant to the University of Manchester.

Manuscript received 25 November 2014 and in revised form 12 May 2015.

Published, JLR Papers in Press, May 31, 2015
DOI 10.1194/jlr.M055772

Abbreviations: 15-PGDH, 15-prostaglandin hydroxydehydrogenase; A-EA, arachidonoyl ethanolamine; AL-EA, α-linolenoyl ethanolamine; COX, cyclooxygenase; DH-EA, docosahexaenoyl ethanolamine; EP-EA, eicosapentaenoyl ethanolamine; FAAH, fatty acid amide hydrolase; FA-EA, fatty acyl ethanolamine; L-EA, linoleoyl ethanolamine; MRM, multiple reaction monitoring; N-AAA, *N*-acylethanolamine-hydrolyzing acid amidase; NAPE, *N*-acyl phosphatidylethanolamine; NArPE, *N*-arachidonoyl phosphatidylethanolamine; O-EA, oleoyl ethanolamine; PC, phosphatidylcholine; P-EA, palmitoyl ethanolamine; PG, prostaglandin; PG-EA, prostaglandin ethanolamine; PGS, prostaglandin synthase; PL, phospholipase; PLD, phospholipase D; ST-EA stearoyl ethanolamine; TX, thromboxane.

[1]To whom correspondence should be addressed.
e-mail: anna.nicolaou@manchester.ac.uk

[S] The online version of this article (available at http://www.jlr.org) contains supplementary data in the form of one figure.

pathways have been carried out in mice and rat tissues, and, interestingly, their prevalence appears to be time and cell specific (15). Finally, A-EA may also be catabolized to arachidonic acid and ethanolamine by fatty acid amide hydrolase (FAAH; EC 3.5.1.99) or *N*-acylethanolamine-hydrolyzing acid amidase (N-AAA) (16, 17) (**Fig. 1**).

Prostamides exhibit a range of activities in various systems. $PGF_{2\alpha}$-EA is involved in inflammatory pain and dorsal horn nociceptive neuron excitability, while PGE_2-EA increases blood flow and reduces mean arterial pressure in the renal medulla, exhibits strong neuroprotective properties in cerebellar neurons, and along with PGD_2-EA, induces apoptosis in an in vitro model of colorectal carcinoma (18–21). Prostamides do not show potent interaction with prostanoid receptors, and studies using isolated feline iris cells have suggested the presence of prostamide-sensitive receptors different from the ones responding to PGs (22–24). The prostamide precursor A-EA has also been shown to exhibit neuroprotective and analgesic roles in inflammation and pain models (25, 26), while topical administration reduces intraocular pressure (27). However, its mode of action is mediated through the CB_1 and CB_2 cannabinoid and vanilloid subtype-1 (TRPV1) receptors that are not activated by prostamides (24, 28). In addition, reports now indicate that NAPEs also have biological functions in their own right, such as membrane stabilization and inhibition of macrophage phagocytosis (29). Consistently, NAPEs have been detected in low abundance in mammalian systems but then accumulate under conditions of cellular stress (e.g., ischemia and inflammation), leading to suggestions of putative protective roles [reviewed in (29, 30)].

Although A-EA has been found in the cornea as a minor lipid (30), neither its metabolism through COX-2 to form prostamides nor the prevalence of its biochemical precursor NArPE have been investigated. In this study, we explored the endogenous production of $PGF_{2\alpha}$-EA, PGE_2-EA, and PGD_2-EA by the cornea and show its capability to form these prostamides when A-EA is added externally. We also present data detailing the levels of A-EA and its congeners, as well as NArPE and other fatty acyl NAPE species in rabbit corneal tissue. Given the pharmacological potency of prostamides in ocular health, detailed information on their profile and biochemical precursors in cornea could provide valuable insight into ocular physiology and potential therapeutics.

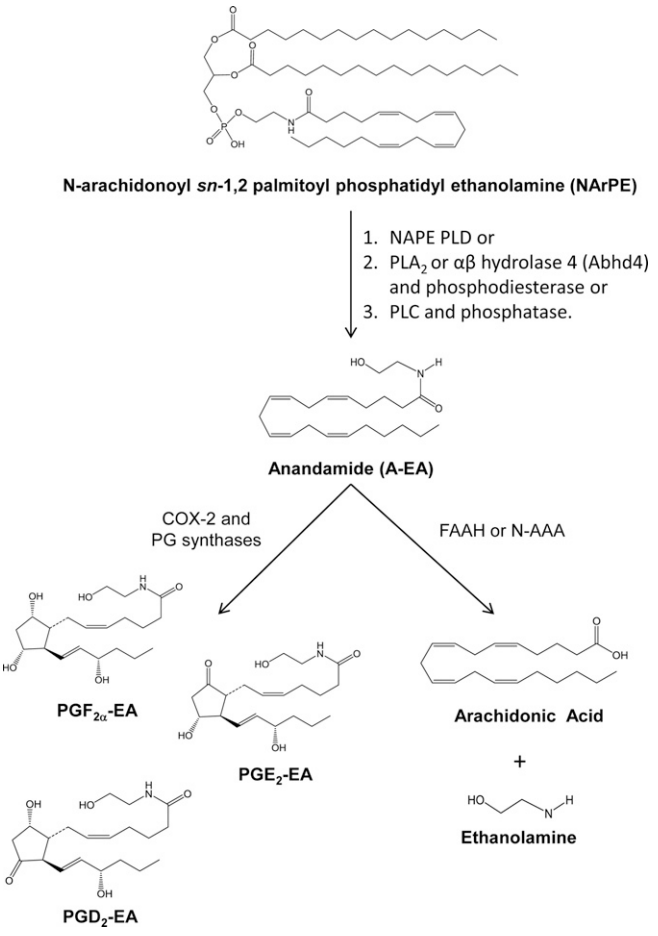

Fig. 1. Schematic overview of prostamide biosynthesis. A-EA is released from NArPE by the action of NAPE-PLD (1), PLA_2 or αβ hydrolase 4 (abhd4) and a metal dependent phosphodiesterase (2), or PLC and phosphatases (3) [e.g., tyrosine phosphatase (PTPN22)]. Subsequently, A-EA is metabolized by COX-2 and PGSs to prostamides such as PGE_2-EA, PGD_2-EA, and $PGF_{2\alpha}$-EA. A-EA can also be hydrolyzed by FAAH or N-AAA to arachidonic acid and ethanolamine.

MATERIALS AND METHODS

Materials

PGE_2, $PGF_{2\alpha}$, PGD_2, 15-deoxy $^{\Delta 12,14}$ PGJ_2, PGJ_2, $^{\Delta 12}PGJ_2$, PGE_3, PGD_3, PGE_1, PGD_1, 13,14 dihydro 15-keto PGE_2, 13,14 dihydro 15-keto $PGF_{2\alpha}$, TXB_2, 6-keto $PGF_{1\alpha}$ PGB_2-*d4*, A-EA, A-EA-*d8*, palmitoyl ethanolamine (P-EA), docosahexaenoyl ethanolamine (DH-EA), α-linolenoyl ethanolamine (AL-EA), oleoyl ethanolamine (O-EA), stearoyl ethanolamine (ST-EA), linoleoyl ethanolamine (L-EA), PGE_2-EA, $PGF_{2\alpha}$-EA, PGD_2-EA, and FAAH inhibitor PF3845 (31) were purchased from Cayman Chemical Co. (Ann Arbor, MI). *N*-arachidonoyl dipalmitoyl phosphatidylethanolamine was purchased from Enzo Life Sciences (Exeter, UK). Security guard cartridges C18 (5 μm, 4 × 2.0 mm), C18-E solid phase extraction cartridges (SPE; 500 mg sorbent), amber glass vials (1.5 ml), insert glass vials (0.15 ml), Teflon septa and lids were from Phenomenex (Macclesfield, UK). Male white New Zealand rabbit corneas were provided by Sera Laboratories International Ltd. (Haywards Heath, UK). Chloroform, methanol, ethanol, acetonitrile, hexane (all HPLC grade), and methyl formate (97% spectroscopy grade) were from Fisher Scientific (Loughborough, UK). HPLC-grade glacial acetic acid, Trizma Base, indomethacin, and protease inhibitor cocktail [4-(2-aminoethyl) benzenesulfonyl fluoride hydrochloride (104 mM), aprotinin (80 μM), bestatin (4 mM), E-64 (1.4 mM), leupeptin (2 mM), pepstatin A (1.5 mM)] were purchased from Sigma-Aldridge (Dorset, UK). EDTA was sourced from BDH (Poole, UK). Ultrapure water was tapped by a MilliQ Gradient system (Millipore, Volketswil, Switzerland).

Tissue homogenization and extraction of prostamides and fatty acid ethanolamines

Rabbit corneas (~75–100 mg each) were individually homogenized, using a glass Dounce tissue grinder (1 ml) (Fisher Scientific) with a tightly fitting pestle, in 1 ml ice-cold Tris-hydrochloride

buffer (100 mM, pH 8 adjusted with 1 M HCl) containing EDTA (1 mM), FAAH inhibitor PF3845 (100 nM), and a protease inhibitor cocktail (1:100 dilution). During homogenization the tissue grinder and homogenate were kept on ice. When endogenous production of prostamides was monitored, corneal tissue homogenates (eight corneas) were pooled. Subsequent ex vivo investigations of prostamide formation were carried out by incubating corneal tissue homogenates (two corneas in 3 ml Tris-hydrochloride buffer) for 10 min at 37°C with exogenously added *a*) A-EA (10 μM, 50 μM), *b*) A-EA (50 μM) with and without indomethacin (3 μM), and *c*) A-EA (50 μM) with and without the FAAH inhibitor PF3845.

Prostamides and fatty acyl ethanolamines (FA-EA) were extracted using chloroform-methanol (2:1, v/v) (32, 33). Specifically, ice-cold chloroform-methanol (9 ml) was added to each corneal tissue homogenate followed by internal standard (A-EA-*d*8, 5 μl as 1 ng/μl in ethanol). The resulting suspensions were kept on ice for 30 min with occasional vortexing. Each sample was vortexed and centrifuged at 4,000 rpm for 8 min to separate the organic and aqueous phases. The organic layer (bottom) from each sample was then removed into a clean wide-neck vial. The pooled supernatant was evaporated under a fine stream of nitrogen, and the remaining residue was reconstituted in 50–100 μl ethanol and stored at −20°C, for no more than 1 week, awaiting LC/ESI-MS/MS analysis.

LC/ESI-MS/MS analysis of prostamides

Analysis and characterization of PG-EA produced by corneal tissue was performed on an electrospray (ESI) tandem quadrupole Xevo TQ-S mass spectrometer (Waters, Elstree, Hertfordshire, UK) coupled to an Acquity Ultrahigh Pressure Liquid Chromatography (UPLC) system. The system was controlled by MassLynx v4.1 Software. TargetLynx was used to construct calibration lines and calculate the concentration of analytes of interest. Optimized ESI-MS/MS conditions were achieved through use of Intellistart within MassLynx software. Individual standards (100 pg/μl) were introduced into the spectrometer by direct infusion via the Xevo TQ-S integrated syringe pump (flow rate 10 μl/min) combined with UPLC solvent flow (rate 0.2 ml/min). All analytes were monitored on the positive ionization mode. Capillary voltage was set at 2,000 V, source temperature at 100°C, desolvation temperature at 400°C, and the cone voltage at 35 V. The collision energy was optimized for each compound to obtain optimum sensitivity using argon as collision gas and was set at 14 eV for PGE_2-EA and PGD_2-EA, and 16 eV for $PGF_{2\alpha}$-EA.

Chromatographic analysis of PG-EA was performed on an Acquity UPLC® BEH Phenyl C18 column (1.7 μm, 2.1 × 50 mm) (Waters) maintained at 25°C supported with Acquity UPLC® BEH Phenyl VanGuard precolumn (1.7 μm, 2.1 × 5 mm) (Waters). Sample injections were performed with the Acquity sample manager (Waters); the sample chamber temperature was set at 8°C, and the injection volume was 3 μl. Analytes were separated using a method comprising two solvents: solvent A, water-glacial acetic acid 99.5:0.5 (v/v); solvent B, acetonitrile-glacial acetic acid 99.5:0.5 (v/v). Prostamides were eluted using an isocratic method of 25.5% solvent B from 0 to 3 min with a flow rate of 0.4 ml/min. At 3.1 min, solvent B was increased to 80% and the flow rate to 0.6 ml/min to wash the column for a further 5 min before returning to the original conditions. Multiple reaction monitoring (MRM) assays were set up using the following transitions: $PGF_{2\alpha}$-EA: *m/z* 380 > 362, 380 > 344, 380 > 283, 380 > 62; PGE_2-EA and PGD_2-EA: *m/z* 378 > 360, 378 > 342, 378 > 299, 378 > 62.

LC/ESI-MS/MS analysis of FA-EAs

LC/ESI-MS/MS analysis of FA-EA was performed on an electrospray (ESI) triple quadrupole Quattro Ultima mass spectrometer (Waters) coupled to a Waters Alliance 2695 HPLC pump. Instrument control and data acquisition were performed using the MassLynx™ V4.0 software. For optimization of ESI/MS and ESI/MS/MS conditions, individual standards (10 ng/μl) were introduced into the spectrometer by direct infusion through a syringe pump (flow rate 10 μl/min) through the HPLC solvent flow (rate 0.2 ml/min). All analytes were monitored on the positive ionization mode. Capillary voltage was set at 3,500 V, source temperature at 100°C, desolvation temperature at 400°C, cone voltage at 35 V, while the collision energy was optimized for each compound using argon as collision gas and was set to the following: P-EA, 13 eV; AL-EA, 14 eV; L-EA, 15 eV; O-EA, 16 eV; ST-EA, 15 eV; eicosapentaenoyl ethanolamine (EP-EA), 15 eV; A-EA, 15 eV; DH-EA, 15 eV; A-EA-*d*8, 16 eV.

Chromatographic analysis of FA-EA species was performed on a Luna C18(2) column (5 μm, 150 × 2.0 mm inner diameter) (Phenomenex, Macclesfield, UK) maintained at ambient temperature. Sample injections were performed with a Waters 2690 autosampler; the sample chamber temperature was set at 8°C. The injection volume was 10 μl, and the flow rate 0.2 ml/min. Analytes were separated using an acetonitrile-based gradient system comprising two solvents; solvent A, acetonitrile-water-glacial acetic acid 2:97.5:0.5 (v/v/v); solvent B, acetonitrile-water-glacial acetic acid 97.5:2:0.5 (v/v/v). The following gradient was used: 0.0–10.00 min, 30% solvent B increasing linearly to 70% solvent B; 10.00–40.00 min 70% solvent B decreasing linearly to 60% solvent B; 40.00–41.00 min 60% solvent B increasing linearly to 90% solvent B; 41.00–55.00 min 90% solvent B; 55.00–56.00 90% solvent B decreasing linearly to 30% solvent B; 56.00–69.00 min 30% solvent B. A shallow gradient was put in place between 10 and 40 min (70% to 60% solvent B) to improve the resolution of FA-EA. MRM assays were set up using the following transitions: P-EA, *m/z* 300 > 62; AL-EA, *m/z* 322 > 62; L-EA, *m/z* 324 > 62; O-EA, *m/z* 326 > 62; ST-EA, *m/z* 328 > 62; EP-EA, *m/z* 346 > 62; A-EA, *m/z* 348 > 62; DH-EA, *m/z* 372 > 62; A-EA-*d*8, *m/z* 356 > 63. Results are expressed as picograms metabolite per milligrams wet tissue, using calibration lines constructed with commercially available standards.

Extraction and LC/ESI-MS/MS analysis of prostanoids

Prostanoids were extracted and analyzed as previously described (34, 35). Briefly, individual corneas were homogenized in 500 μl of ice-cold 15% methanol (v/v) using PGB_2-*d4* (40 μl of a 1 ng/μl ethanol solution) as internal standard. The homogenates were acidified to pH 3.0 with 1 M hydrochloric acid, semipurified using SPE and eluted with methyl formate. The solvent was then evaporated under nitrogen, and the lipid residue reconstituted in 100 μl ethanol and stored at −20°C. LC/ESI-MS/MS analysis of prostanoids was based on MRM assays using the following transitions: 15-deoxy $\Delta^{12,14}$ PGJ_2, *m/z* 315 > 271; PGJ_2, *m/z* 333 > 271; Δ^{12} PGJ_2, *m/z* 333 > 271; PGE_3, *m/z* 349 > 269; PGD_3, *m/z* 349 > 269; PGE_2, *m/z* 351 > 271; PGD_2, *m/z* 351 > 271; 13,14-dihydro 15-keto PGE_2, *m/z* 351 > 333; 13,14-dihydro 15-keto $PGF_{2\alpha}$, *m/z* 353 > 113; $PGF_{2\alpha}$, *m/z* 353 > 193; PGE_1, *m/z* 353 > 317; PGD_1, *m/z* 353 > 317; 6-keto $PGF_{1\alpha}$, *m/z* 369 > 163; TXB_2, *m/z* 369 > 169; PGB_2-*d4*, *m/z* 337 > 174. Results are expressed as picograms metabolite per milligrams wet tissue, using calibration lines constructed with commercially available prostanoid standards.

Extraction and ESI-MS/MS analysis of NAPE species

Two corneas were homogenized individually, using a glass Dounce tissue grinder (1 ml) in ice-cold chloroform-methanol (2:1, v/v) (0.5 ml aliquots to a volume of 3 ml per cornea). The sample was then kept on ice for 90 min with occasional vortexing. Water (0.5 ml) was added to each sample and the vials vortexed before being centrifuged at 5,000 rpm for 8 min to separate the organic and aqueous phases. The organic layer (bottom) from

each sample was then removed and pooled into a clean wide-neck vial, and the solvent evaporated under a fine stream of nitrogen. The lipid residue was reconstituted in 100 μl chloroform-methanol (1:4, v/v) and stored at −20°C awaiting ESI-MS/MS analysis (36).

In order to optimize the ESI-MS and ESI-MS/MS conditions for NAPE analysis, commercially available *N*-arachidonoyl dipalmitoyl phosphatidyl ethanolamine was used. Using direct infusion (flow rate 10 μl/min), the optimum collision energy was found to be 40 eV, using argon as collision gas. The analyte was monitored on negative ionization mode and was found to fragment in a similar way to previously published data (36). The corneal extract was diluted 1:10 (v/v) with chloroform-methanol-water-acetic acid (2: 6.95:1:0.05, v/v/v/v) and analyzed through direct infusion. ESI-MS spectra were recorded over the range *m/z* 800–1,250. Ions with *m/z* $[M-H]^-$ corresponding to NArPE and NAPE were further analyzed by ESI-MS/MS to confirm their identity and obtain information on the *sn*-1 and *sn*-2 acyl chains.

RESULTS

LC/ESI-MS/MS analysis of prostamides in rabbit cornea

The ESI-MS, MS/MS spectra and fragmentation patterns of prostamides $PGF_{2\alpha}$-EA, PGE_2-EA, and PGD_2-EA were studied using commercially available standards (**Fig. 2**). All prostamide standards were found to form stable sodiated

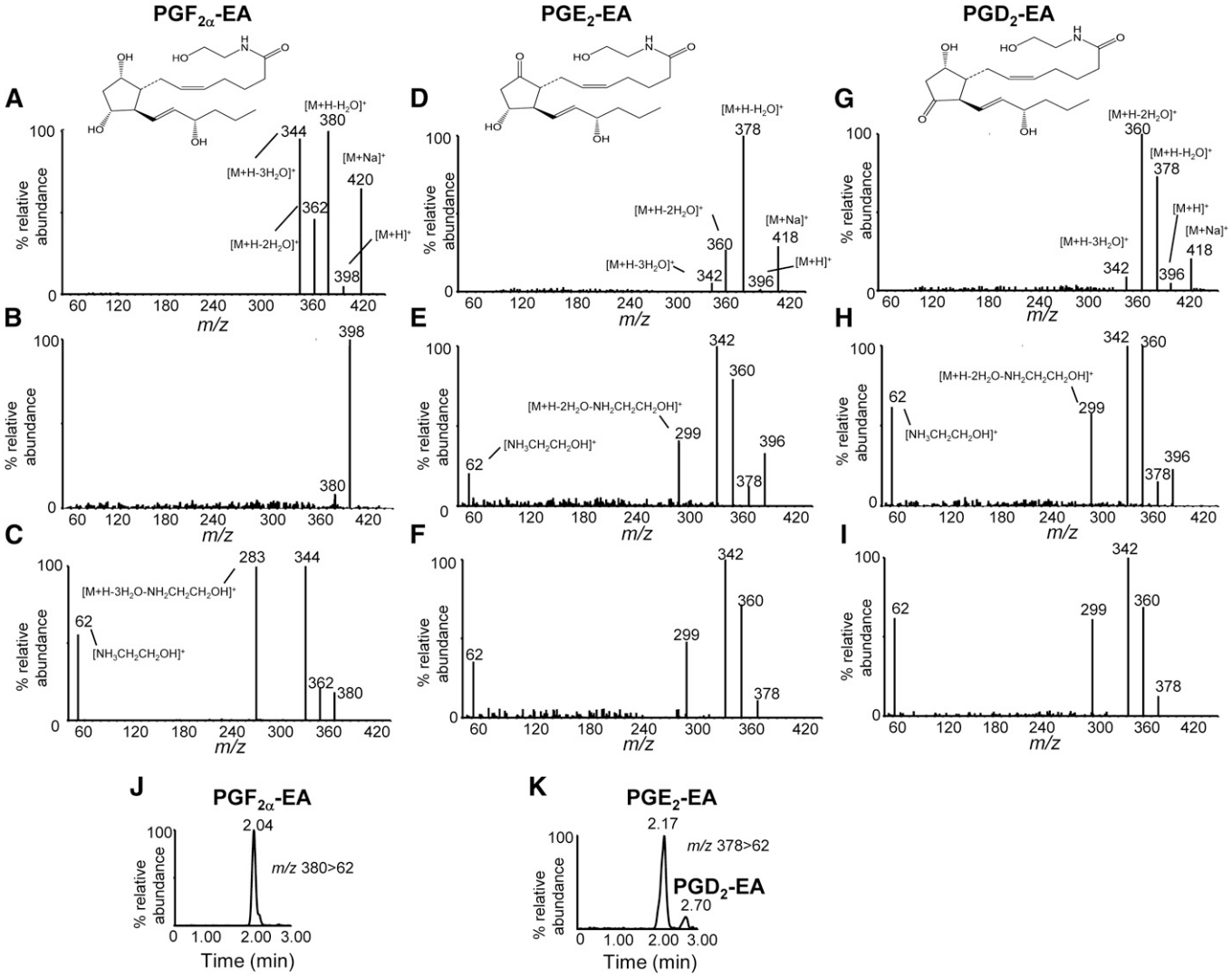

Fig. 2. Analysis of prostamide standards $PGF_{2\alpha}$-EA, PGE_2-EA, and PGD_2-EA. The ESI-MS spectrum of $PGF_{2\alpha}$-EA standard (A) shows that the sodium adduct $[M+Na]^+$ *m/z* 420 and $[M+H-H_2O]^+$ *m/z* 380 are readily formed; while $[M+H]^+$ *m/z* 398 is found at extremely low levels and was not easy to fragment (B), product ion scan of $[M+H-H_2O]^+$ *m/z* 380 (C) indicates that the dehydration products *m/z* 362 and 344, and specific fragments *m/z* 283 and 62, can be used for the detection and quantitation of $PGF_{2\alpha}$-EA. The ESI-MS spectrum of PGE_2-EA standard shows the formation of sodiated ion $[M+Na]^+$ *m/z* 418 (D) and low prevalence of $[M+H]^+$ *m/z* 396, while product ion scans of $[M+H]^+$ *m/z* 396 (E) and $[M+H-H_2O]^+$ *m/z* 378 (F) show the dehydration products *m/z* 360 and 342, and specific fragments *m/z* 299 and 62, that can be used for the detection and quantitation of PGE_2-EA. The ESI-MS spectra of the PGD_2-EA standard show the formation of the sodiated, dehydration, and specific fragment ions identical to the ones produced by PGE_2-EA (G, H, and I). Sample LC/ESI-MS/MS reconstructed ion chromatograms of prostamides $PGF_{2\alpha}$-EA (J) and PGE_2-EA and PGD_2-EA (K) using the following MRM transitions: *m/z* 380 > 62 and 378 > 62 (all analytes at 10 pg/μl); chromatographic conditions are described in Materials and Methods. Commercially available standards were used.

ions $[M+Na]^+$ *m/z* 420 for $PGF_{2\alpha}$-EA, and *m/z* 418 for both PGE_2-EA and PGD_2-EA, possibly reflecting their storage in glass vials. Notably, the relative abundance of $[M+H]^+$ species (*m/z* 398 for $PGF_{2\alpha}$-EA, and *m/z* 396 for both PGE_2-EA and PGD_2-EA) was found to be very low (Fig. 2A, D, G, respectively), and, for all prostamides examined here, the predominant ions corresponded to $[M+H-H_2O]^+$ (*m/z* 380 for $PGF_{2\alpha}$-EA and *m/z* 378 for PGE_2-EA and PGD_2-EA). Further fragmentation of $[M+H-H_2O]^+$ ions resulted in the product ions $[M+H-2H_2O]^+$ *m/z* 362, $[M+H-3H_2O]^+$ *m/z* 344, and $[M+H-3H_2O-NH_2CH_2CH_2OH]^+$ *m/z* 283 for $PGF_{2\alpha}$-EA (Fig. 2C), and $[M+H-2H_2O]^+$ *m/z* 360, $[M+H-3H_2O]^+$ *m/z* 342, and $[M+H-2H_2O-NH_2CH_2CH_2OH]^+$ *m/z* 299 for PGE_2-EA and PGD_2-EA (Fig. 2F, I). The protonated 2-amino ethanol ion $[NH_3CH_2CH_2OH]^+$ *m/z* 62, characteristic of ethanolamine metabolites, was also detected following fragmentation of $[M+H]^+$ (PGE_2-EA and PGD_2-EA; Fig. 2E, H) and $[M+H-H_2O]^+$ ($PGF_{2\alpha}$-EA, PGE_2-EA, and PGD_2-EA; Fig. 2C, F, I). All these findings are in agreement with previously published data on the prostamide formation and identification in vitro and FAAH knockout mice (10, 12, 13, 37).

Although sodium adducts have been used to analyze $PGF_{2\alpha}$-EA (21), prostamide adducts proved to be very stable under our experimental conditions, and the collision energies required were found too high (>40 eV) to produce identifiable characteristic fragments. Furthermore, under our experimental setting the prostamide standards were readily dehydrated resulting in a very low abundance of the $[M+H]^+$ ions (Fig. 2A, D, G), and it was necessary to use very high concentrations of the commercially available standard (>40 ng on the column) in order to detect these parent ions. Therefore, in order to set up an LC/ESI-MS/MS assay appropriate for detection and quantitation of prostamides found at low concentrations in biological samples, we followed the fragmentation of $[M+H-H_2O]^+$ ions using four MRM transitions: $PGF_{2\alpha}$-EA, *m/z* 380 > 362, 380 > 344, 380 > 283, and 380 > 62; PGE_2-EA and PGD_2-EA, *m/z* 378 > 360, 378 > 342, 378 > 299, and 378 > 62. Chromatographic separation of $PGF_{2\alpha}$-EA, PGE_2-EA, and PGD_2-EA was achieved using a reverse phase C18 column with an acidified acetonitrile-based gradient system (Fig. 2J, K). Analysis of rabbit corneal tissue extracts using this assay did not offer conclusive evidence for the presence of $PGF_{2\alpha}$-EA, PGE_2-EA, and PGD_2-EA (**Fig. 3**).

Further experiments were designed to explore the capability of rabbit cornea to form prostamides. For this, tissue homogenates were incubated with exogenously added A-EA (10 and 50 μM) (**Fig. 4**). The LC-MS/MS reconstructed ion chromatograms presented in Fig. 4A–D show increased production of $PGF_{2\alpha}$-EA in all transitions recorded and following incubation with 50 μM A-EA. The ESI-MS/MS spectrum of the compound eluted at 2.14 min (retention time of the $PGF_{2\alpha}$-EA standard) confirms the presence of $PGF_{2\alpha}$-EA in the A-EA-treated corneal extract (Fig. 4E). Furthermore, when the tissue homogenate was incubated with A-EA (50 μM) in the presence of the COX inhibitor indomethacin, $PGF_{2\alpha}$-EA formation was inhibited by ~70% (**Fig. 5A**, B), while the presence of the FAAH inhibitor PF3845 showed a clear increase in $PGF_{2\alpha}$-EA production (~65%) (**Fig. 6A**, B). For clarity, Figs. 5 and 6 show two of the four recorded transitions (i.e., *m/z* 380 > 62 and 380 > 283), the ones that gave the best signal when examining the A-EA-supplemented corneal extract and confirm the presence of 2-amino ethanol (Fig. 4).

The LC/ESI-MS/MS reconstructed ion chromatograms presented in Fig. 4F–I suggest that the A-EA-supplemented corneal extracts produce PGE_2-EA and PGD_2-EA, albeit at very low levels. The presence of these compounds is further supported by the product ion spectra corresponding to peaks eluted at 2.24 and 2.79 min, the retention times of PGE_2-EA and PGD_2-EA authentic standards, respectively (Fig. 4J, K). Inhibition of COX by indomethacin showed reduction of the putative PGE_2-EA and PGD_2-EA peaks (~30–70%; peaks eluting at 2.23 and 2.79 min, respectively; Fig. 5C, D), while inhibition of FAAH appeared to increase the corresponding signals (~30–60%) (Fig. 6C, D), further supporting the identification.

Treatment with indomethacin reduced the relative production of peaks eluting at retention times earlier than that of $PGF_{2\alpha}$-EA indicating the possible presence of 6-keto $PGF_{1\alpha}$-EA, the stable metabolite of prostacyclin ethanolamine (PGI_2), in the corneal tissue (11). A single ion recording (SIR) for $[M+H]^+$ *m/z* 414 revealed two broad peaks at retention times 0.56 and 1.27 min, respectively (supplementary Fig. 1). Furthermore, an MRM experiment based on the dehydrated ions $[M+H-H_20]^+$ *m/z* 396, $[M+H-2H_20]^+$ *m/z* 378, and $[M+H-3H_20]^+$ *m/z* 360, as well as the protonated 2-amino ethanol ion $[NH_3CH_2CH_2OH]^+$ *m/z* 62 (*m/z* 414 > 396, 414 > 378, 414 > 360, and 414 > 62), suggested the presence of these 6-keto $PGF_{1\alpha}$-EA-related ions at retention times 0.61 min and 1.32 min, while indomethacin appeared to reduce the formation of only one of the observed peaks (retention time 1.22 min; supplementary Fig. 1D–H). These findings indicate the putative formation of 6-keto $PGF_{1\alpha}$-EA by corneal tissue, although a synthetic standard would be needed to further explore and confirm this finding.

LC/ESI-MS/MS analysis of prostanoids in rabbit cornea

Although A-EA is the substrate for enzymatic conversion by COX-2 to PGH_2-EA (13), it is the expression and activity of the individual PGSs that ultimately determines the tissue profile of prostamides. We have, therefore, assessed the profile of prostanoids in rabbit cornea as means of appreciating the range and relative activity of PGSs in this tissue. Prostacyclin (PGI_2, measured as 6-keto $PGF_{1\alpha}$; **Table 1**) appeared to be the predominant prostanoid produced at 270.9 ± 109.8 pg/mg tissue, while $PGF_{2\alpha}$, PGE_2, and PGD_2 were produced at lower levels (40.5 ± 15.0, 151.9 ± 103.5, and 187.1 ± 73.4 pg/mg tissue, respectively) (**Table 2**). Interestingly, PGE_1 and PGD_1, and PGE_3 and PGD_3, derived from COX metabolism of dihomo γ-linolenic acid (20:3) and EPA (20:5) respectively, were also detected albeit at very low levels (0.9–5.3 pg/mg tissue). Furthemore, the cyclopentanone PGs PGJ_2, $\Delta^{12}PGJ_2$, and 15 deoxy $\Delta^{12,14}$ PGJ_2 were also detected at 3–47 pg/mg tissue, showing that PGD_2 may also act as precursor to anti-inflammatory species in the cornea.

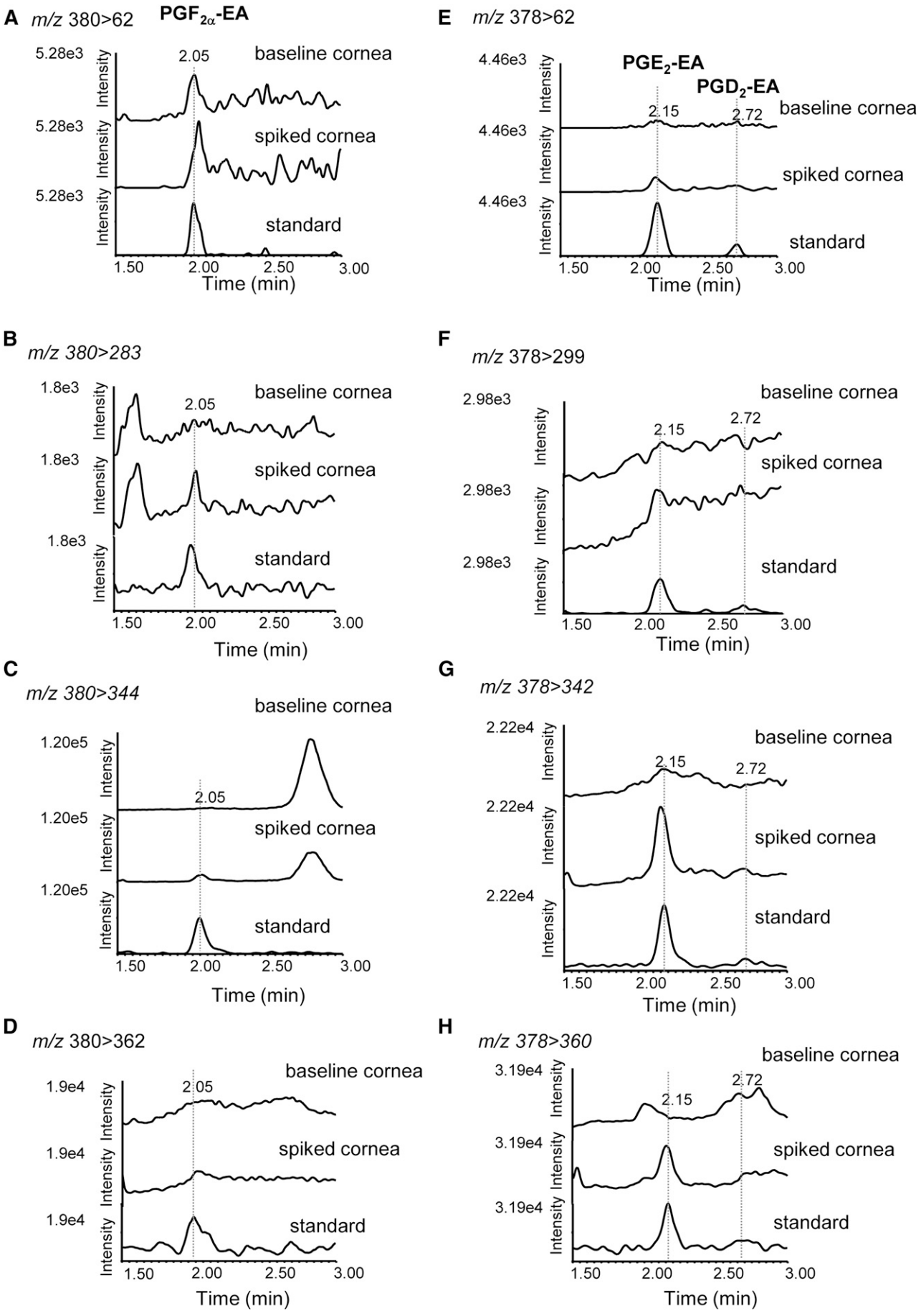
A
m/z 380>62
PGF2α-EA
baseline cornea
spiked cornea
standard
2.05
Intensity
Time (min)
B
m/z 380>283
C
m/z 380>344
D
m/z 380>362
E
m/z 378>62
PGE2-EA
PGD2-EA
2.15
2.72
F
m/z 378>299
G
m/z 378>342
H
m/z 378>360

Finally, the presence of 13,14 dihydro 15-keto metabolites of PGE_2 and $PGF_{2\alpha}$ shows the expression of 15-prostaglandin dehydrogenase (15-PGDH) and PG keto reductases in rabbit cornea, suggesting that the tissue actively controls the levels of PGs through their metabolism and deactivation (38). Overall, these data clearly show the presence of an active arachidonic acid cascade through COX, while the PG profile suggests the prevalence of PGIS, PGES, and PGDS isoforms in rabbit cornea, suggesting that the tissue has the capability of forming the correspondent prostamide species.

LC/ESI-MS/MS analysis of FA-EAs in rabbit cornea

Tissue levels of prostamides depend on the availability of A-EA; thus, a low corneal A-EA level could explain the lack of detectable levels of $PGF_{2\alpha}$-EA, PGE_2-EA, and PGD_2-EA in baseline corneal extracts. This was confirmed by LC/ESI-MS/MS analysis of the corneal extract and showed A-EA at 10.7 ± 5.0 pg/mg tissue. Overall, seven species of FA-EA were detected in rabbit cornea; the level of A-EA was similar to ST-EA (8.3 ± 4.9 pg/mg tissue) and L-EA (13.8 ± 4.2 pg/mg tissue), but lower than P-EA (32.7 ± 12.5 pg/mg tissue) and O-EA (42.1 ± 26.8 pg/mg tissue), while AL-EA and DH-EA were detected at much lower concentrations (0.4 ± 0.1 and 0.7 ± 0.3 pg/mg tissue, respectively); data shown in **Fig. 7**.

Analysis of NAPEs in rabbit cornea

The pool of A-EA and congeners is derived from membrane stores of the respective NAPE. Commercially available *N*-arachidonoyl dipalmitoyl phosphatidyl ethanolamine (978 Da) was used to optimize the experimental conditions for the ESI-MS/MS analysis of NAPE species by direct infusion. Fragmentation of $[M\text{-}H]^-$ *m/z* 977 resulted in an abundant product ion *m/z* 255, which was attributed to the carboxylate anion derived from the fatty acyl in position *sn*-2 (i.e., palmitate), while other product ions were identified as the *sn*-2 *N*-acyl lysophospholipid *m/z* 739, *N*-arachidonoyl ethanolamide cyclic phosphate derivative *m/z* 482, and *N*-arachidonoylethanolamine phosphate *m/z* 426. These data were in agreement with results published by Astarita et al. (36). A general scan in the range of *m/z* 850–1200 indicated more than 25 potential NAPE species present in corneal lipid extracts. Following a focused MS/MS analysis of the species found in higher abundance (i.e., exceeding 10^7 ion intensity), five NAPE precursor ions with *m/z* 1041, 1083, 1097, 1055, and 1027 were identified (Table 2). These ions are consistent with the expected masses of seen NAPE species (namely, P-EA, AL-EA, L-EA, O-EA, ST-EA, A-EA, and DH-EA NAPE) precursors of the main FA-EA identified in rabbit cornea (Table 2 and Fig. 7).

DISCUSSION

Prostamides and their biochemical precursor A-EA exhibit a range of pharmacological and physiological functions that make them an attractive basis for therapeutic intervention. Nevertheless, there is very little information available that describes endogenous prostamide levels and their biosynthetic formation pathway(s). In particular, there is a complete absence of any comprehensive analyses of biosynthetic pathways to the prostamides upstream of A-EA. The authors believe that this is the first report of such an investigative lipidomic analysis of prostamide formation in a tissue. Beyond prostamides, these studies also incorporated analytic detection of other FA-EAs. The function of these species concurrently detected with A-EA may form a foundation for a more complete investigation of biolipid function in the cornea and anatomically adjacent ocular tissues.

LC/ESI-MS/MS lipidomic analysis of rabbit corneal lipid extract did not provide clear evidence for the presence of endogenous prostamides. The identification was based on four fragment ions per compound, selected for increased sensitivity and corresponding to dehydrated and structure specific ions such as the diagnostic for 2-amino alcohols ion *m/z* 62 (Fig. 2). Although some peaks with retention times similar to the ones of commercially available $PGF_{2\alpha}$-EA, PGE_2-EA, and PGD_2-EA standards were detected, the presence of weak broad signals did not support their identification (Fig. 3). Therefore, evidence of the corneal tissue capability to produce prostamides was sought using externally added A-EA. The formation of $PGF_{2\alpha}$-EA increased following incubation with A-EA, and this production was found to be reduced when COX was inhibited and stimulated by FAAH inhibition. PGE_2-EA and PGD_2-EA showed the same response although they were produced at lower levels than $PGF_{2\alpha}$-EA.

Anandamide as well as L-EA and ST-EA were found at relatively low levels (10.7 ± 5 pg/mg, 13.8 ± 4.2 pg/mg, and 8.3 ± 4.9 pg/mg tissue, respectively) and were not the most abundant of the seven species of FA-EA identified: O-EA and P-EA were found at higher levels (42.1 ± 26.8 and 32.7 ± 12.5 pg/mg tissue, respectively) (Fig. 7). This could be attributed to the higher prevalence of their respective fatty acids at position *sn*-1 of the phosphatidylcholine (PC) precursor (39). DH-EA and AL-EA were minor congeners (0.4 and 0.7 pg/mg tissue, respectively), indicating very low levels of DHA and α-linolenic incorporation at the *sn*-1 position of corneal PC available for transacylation to the amine terminal of phosphatidylethanolamine (PE) (40). This is in contrast to the high levels of di-docosahexanoyl-PC and -PE species reported in rat and bovine retinal phospholipids (41, 42) and highlights

Fig. 3. LC/ESI-MS/MS analysis of prostamides $PGF_{2\alpha}$-EA, PGE_2-EA, and PGD_2-EA in rabbit cornea. Sample reconstructed ion chromatograms of untreated corneal extract (baseline cornea) compared with corneal extract spiked with commercially available prostamide standards (spiked cornea) and standards (standard) at the following MRM transitions: $PGF_{2\alpha}$-EA (retention time 2.05 min): *m/z* 380 > 62 (A), *m/z* 380 > 283 (B), *m/z* 380 > 344 (C), and *m/z* 380 > 362 (D). PGE_2-EA and PGD_2-EA (retention times 2.15 min and 2.72 min, respectively): *m/z* 378 > 62 (E), *m/z* 378 > 299 (F), *m/z* 378 > 342 (G), and *m/z* 378 > 360 (H).

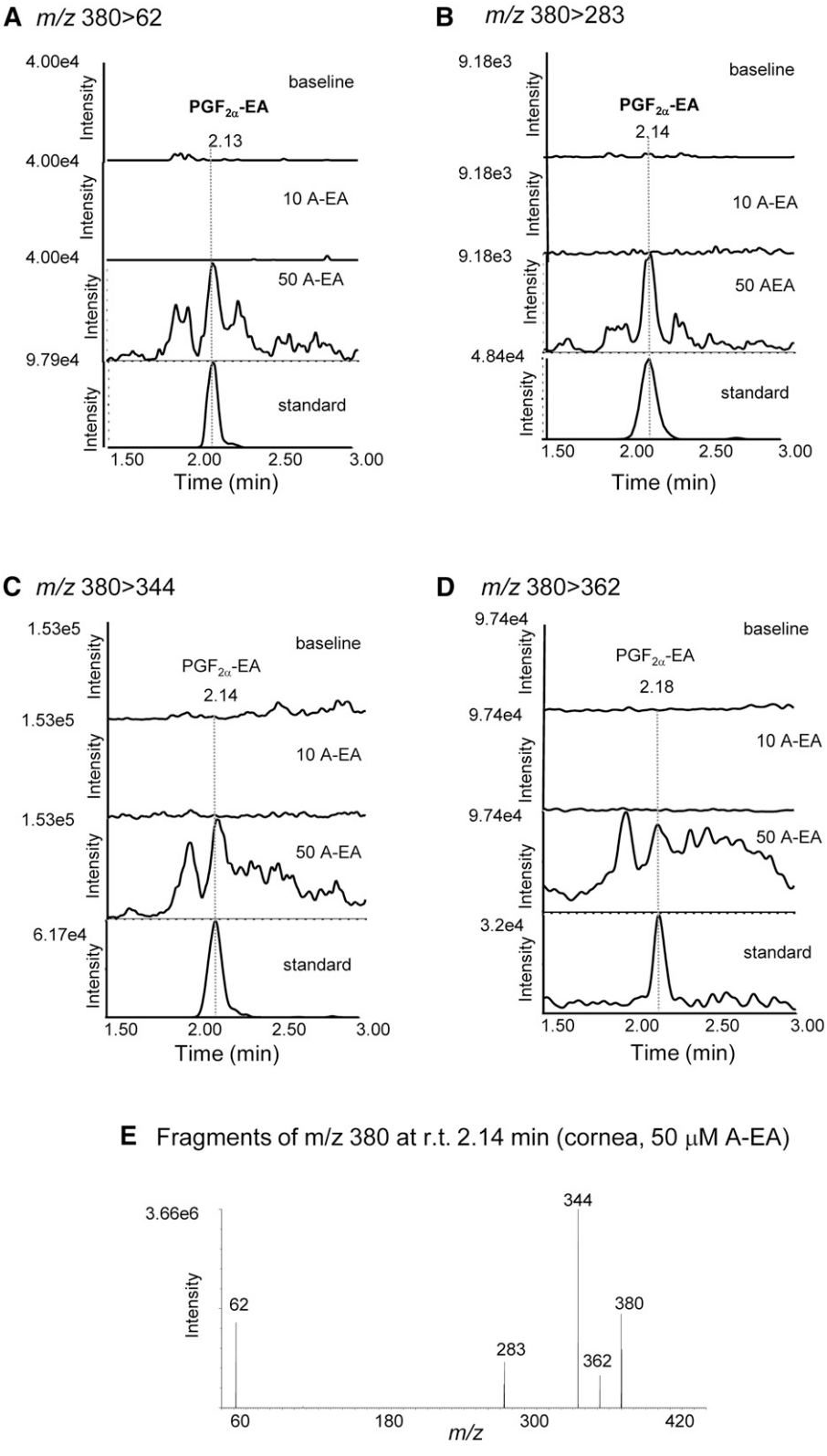

Fig. 4. Confirmation of rabbit corneal tissue capability to produce the prostamides $PGF_{2\alpha}$-EA, PGE_2-EA, and PGD_2-EA. Sample reconstructed ion chromatograms of corneal homogenate incubated (10 min at 37°C) with externally added anandamide (10 μM and 50 μM; 10 A-EA and 50 A-EA) compared with commercially available prostamide standards (standard) at the following MRM transitions: $PGF_{2\alpha}$-EA: *m/z* 380 > 62 (A), *m/z* 380 > 283 (B), *m/z* 380 > 344 (C), and *m/z* 380 > 362 (D). E: Product ions of *m/z* 380 corresponding to the corneal extract peak eluted at retention time (r.t.) 2.14 min ($PGF_{2\alpha}$-EA). PGE_2-EA and PGD_2-EA: *m/z* 378 > 62 (F); *m/z* 378 > 299 (G); *m/z* 378 > 342 (H); and *m/z* 378 > 360 (I). J, K: Product ions of *m/z* 378 corresponding to the corneal extract peak eluted at retention times (r.t.) 2.24 min (PGE_2-EA) and 2.79 (PGD_2-EA).

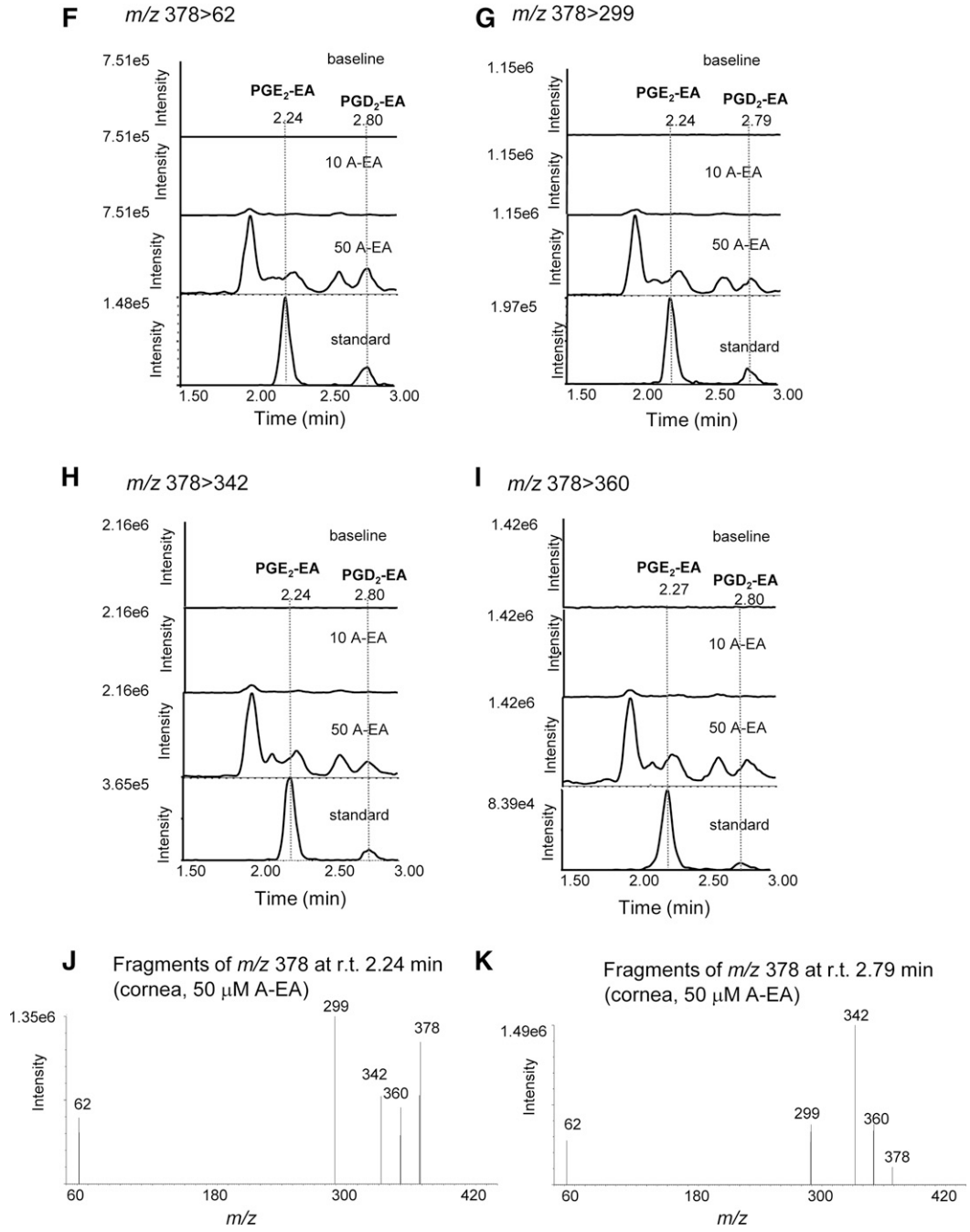

Fig. 4. Continued.

the tissue specific distribution of *sn*-1 docosahexanoyl species of PC (43).

Although A-EA is considered a minor lipid species, representing only 1–10% of total FA-EA in human membranes under basal conditions, studies carried out in brain and nervous tissue indicate A-EA levels are increased in response to injury (44, 45), and that A-EA participates as an anti-inflammatory agent of the immune response (25, 46). Few studies have examined the actions of A-EA per se in the cornea; however, it is a highly innervated tissue, and CB_1 receptors expressed on corneal sensory nerves stimulated by an agonist were found to support a role in contributing to antinociception in the anterior eye (47). Also, in a wound-healing model, both CB_1 and TRPV1 receptor activation increased proliferation and migration in corneal epithelial cells (48, 49), thereby indirectly associating A-EA with these physiological functions. The presence of O-EA, ST-EA, L-EA, and DH-EA was previously unreported in corneal tissue (50). Reports showing a difference in the levels and distribution of 2-AG, A-EA, and P-EA in normal and glaucomatous ocular tissue, from human donors, suggest a role of these fatty acyl moieties in this disease state. The function of other FA-EA species is under investigation and effects on sleeping pattern, appetite control, and depression have been published to date (51–53). EP-EA was not detected in the cornea, which was unsurprising as eicosapentaenoic acid is a

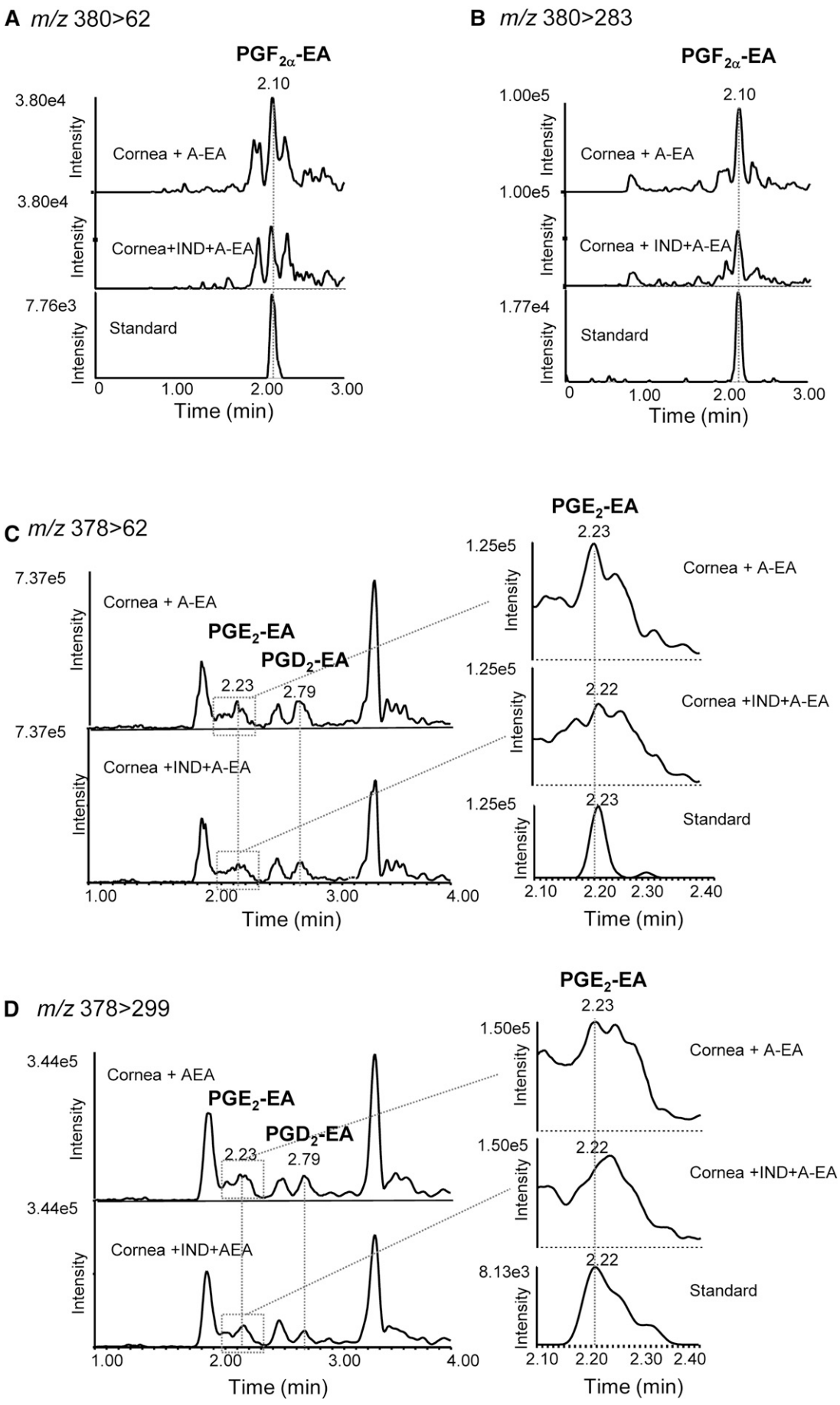
A m/z 380>62
PGF2α-EA
2.10
3.80e4
Intensity
Cornea + A-EA
3.80e4
Intensity
Cornea+IND+A-EA
7.76e3
Intensity
Standard
0
1.00
2.00
3.00
Time (min)
B m/z 380>283
PGF2α-EA
2.10
1.00e5
Intensity
Cornea + A-EA
1.00e5
Intensity
Cornea + IND+A-EA
1.77e4
Intensity
Standard
0
1.00
2.00
3.00
Time (min)
C m/z 378>62
PGE2-EA
7.37e5
Intensity
Cornea + A-EA
PGE2-EA
PGD2-EA
2.23
2.79
7.37e5
Intensity
Cornea +IND+A-EA
1.00
2.00
3.00
4.00
Time (min)
PGE2-EA
2.23
1.25e5
Intensity
Cornea + A-EA
1.25e5
Intensity
2.22
Cornea +IND+A-EA
1.25e5
Intensity
2.23
Standard
2.10
2.20
2.30
2.40
Time (min)
D m/z 378>299
3.44e5
Intensity
Cornea + AEA
PGE2-EA
PGD2-EA
2.23
2.79
3.44e5
Intensity
Cornea +IND+AEA
1.00
2.00
3.00
4.00
Time (min)
PGE2-EA
2.23
1.50e5
Intensity
Cornea + A-EA
1.50e5
Intensity
2.22
Cornea +IND+A-EA
8.13e3
Intensity
2.22
Standard
2.10
2.20
2.30
2.40
Time (min)

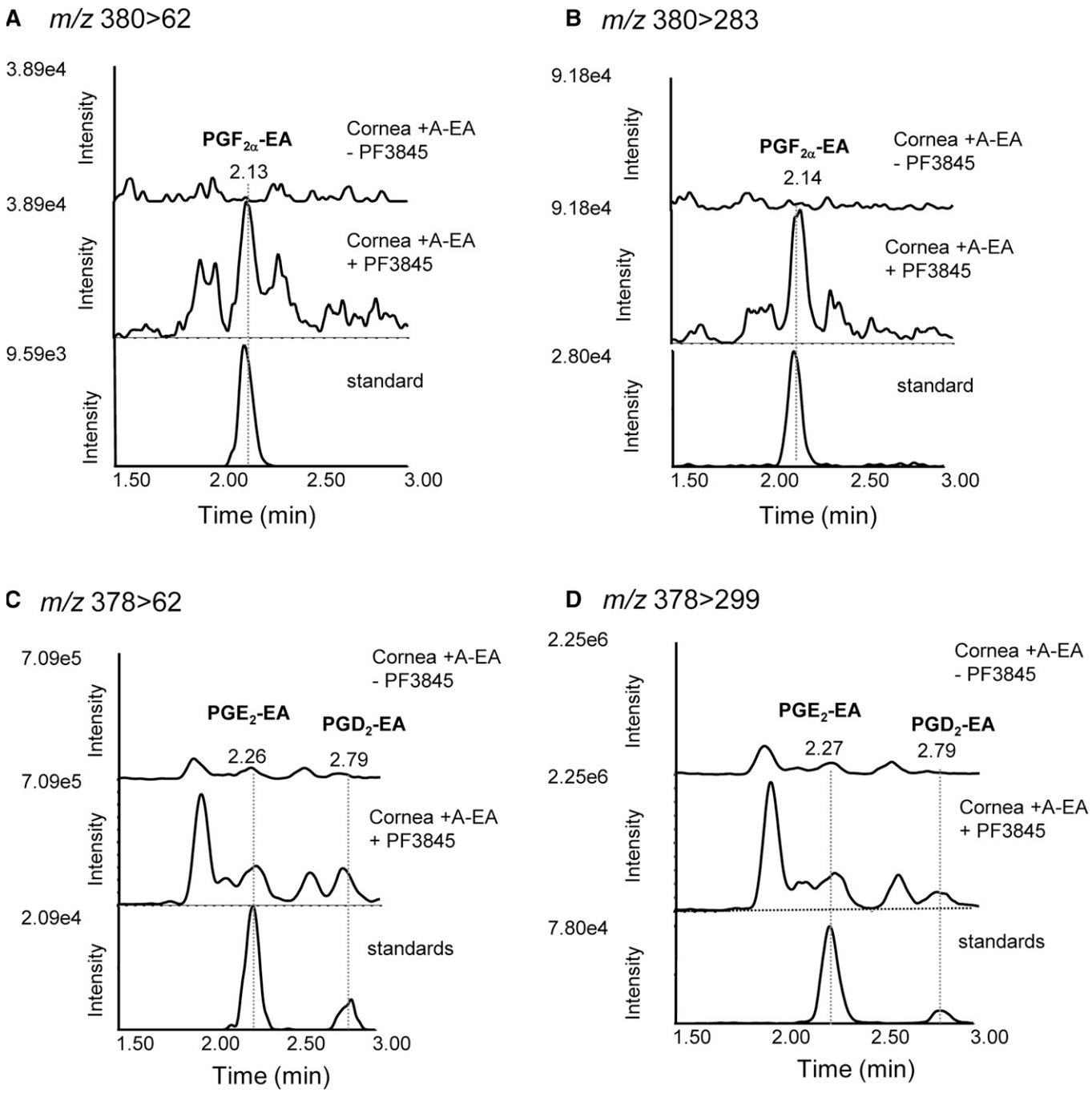

Fig. 6. The effect of FAAH inhibition on the formation of prostamides $PGF_{2\alpha}$-EA, PGE_2-EA, and PGD_2-EA by rabbit corneal tissue. Sample reconstructed ion chromatograms of corneal extract incubated with exogenously added anandamide (50 μM, 10 min at 37°C) in the absence (cornea + A-EA − PF3845) or presence (cornea + A-EA+ PF3845) of the FAAH inhibitor PF3845 (100 nM) compared with commercially available prostamide standards (standard) at the following MRM transitions: $PGF_{2\alpha}$-EA: *m/z* 380 > 62 (A) and *m/z* 380 > 283 (B); PGE_2-EA and PGD_2-EA: *m/z* 378 > 62 (C) and *m/z* 378 > 299 (D).

minor species and DHA is the predominant omega-3 fatty acid found in the brain and ocular tissues (41, 54).

Inactivation of A-EA and other FA-EA occurs through hydrolysis via FAAH and N-AAA. Interestingly, these enzymes possess no sequence homology and are optimally active under basic and acidic conditions respectively, as also reflected in their intracellular localization with FAAH found in membrane fractions and N-AAA in lysosomes

Fig. 5. The effect of COX inhibition on the formation of prostamides $PGF_{2\alpha}$-EA, PGE_2-EA, and PGD_2-EA by rabbit corneal tissue. Sample reconstructed ion chromatograms of corneal extract incubated with exogenously added anandamide (50 μM, 10 min at 37°C) in the absence (cornea + A-EA) or presence of indomethacin (IND, 3 μM) (cornea + IND-A-EA) compared with commercially available prostamide standards (standard) at the following MRM transitions: $PGF_{2\alpha}$-EA: *m/z* 380 > 62 (A) and *m/z* 380 > 283 (B); PGE_2-EA and PGD_2-EA: *m/z* 378 > 62 (C) and *m/z* 378 > 299 (D).

TABLE 1. Prostanoid production by rabbit cornea as estimated by LC/ESI-MS/MS

Compound	MRM (*m/z*)	Amount pg/mg Tissue
15-deoxy $\Delta^{12,14}$ PGJ_2	315 > 271	3.4 ± 3.9
PGJ_2	333 > 271	47.0 ± 23.6
Δ^{12} PGJ_2	333 > 271	14.4 ± 17.5
PGE_3	349 > 269	1.0 ± 0.8
PGD_3	349 > 269	0.9 ± 0.1
PGE_2	351 > 271	151.9 ± 103.5
PGD_2	351 > 271	187.1 ± 73.4
13,14 dihydro 15-keto PGE_2	351 > 333	20.2 ± 15.2
13,14 dihydro 15-keto $PGF_{2\alpha}$	353 > 113	12.6 ± 2.7
$PGF_{2\alpha}$	353 > 193	40.5 ± 15.0
PGE_1	353 > 317	3.0 ± 3.2
PGD_1	353 > 317	5.3 ± 0.6
6-keto $PGF_{1\alpha}$	369 > 163	270.9 ± 109.8
TXB_2	369 > 169	2.0 ± 1.3

Results are expressed as mean ± SD (n = 3 separate experiments).

(17). The therapeutic potential of increasing in situ levels of A-EA has been shown in several studies through the use of FAAH inhibitors (26, 31). The use of nonsteroidal anti-inflammatory drugs (NSAIDs) is also of interest in controlling A-EA levels, with reports suggesting that lower concentrations of NSAIDs are required for the inhibition of A-EA cyclooxygenation than those required for arachidonic acid cyclooxygenation (55, 56). This would allow for a mechanism that modulates endocannabinoid levels without disrupting the effect of PGs.

While multiple pathways exist for generating free FA-EA from membrane stores (15), the precursor NAPE species represent only a minor class of lipids, making up just 0.01% of total animal membrane phospholipids, under physiological conditions (29). Nevertheless, NAPE species are reported to exert bioactive functions independent of being the precursor of the FA-EA [reviewed in (30)]. Concentration of NAPE species can vary greatly depending on the tissue analyzed (e.g., levels described in the rat kidney are 6-fold higher than in rat brain cortex) (57, 58). In the present study, we have identified several NArPE and NAPE species present in corneal tissue (Table 2), and further studies are required to address the pathway of FA-EA generation from these parent phospholipids. Their effects on corneal tissue and cells, per se, also remain to be studied.

The data presented herein suggest that $PGF_{2\alpha}$-EA, PGE_2-EA, and PGD_2-EA can be produced by corneal tissue, a finding that could be attributed to the specific profile of prostanoid synthases expressed in rabbit cornea. To assess this, we analyzed corneal PGs and found that PGI_2 was the most prevalent metabolite, followed by PGE_2 and PGD_2 in approximately equal concentrations, and, at even lower levels, $PGF_{2\alpha}$. It would follow that the most prevalent PG-EA produced by the cornea would be PGI_2-EA, and evidence for its biosynthesis from PGH_2-EA has been presented by Kozak et al. (11). We have explored the possible production of PGI_2-EA through formation of its stable metabolite 6-keto $PGF_{1\alpha}$-EA, using SIR of $[M+H]^+$ *m/z* 414 and fragment ions predicted based on the fragmentation patterns of other prostamides (e.g., dehydration,

TABLE 2. NAPE species in rabbit cornea, as identified by ESI-MS/MS

NAPE $[M-H]^-$ (*m/z*)		*sn*-1 Acyl (*m/z*): (*sn*-1 FA)	*sn*-2 Acyl (*m/z*): (sn-2 FA)	*sn*-2 Lyso NAPE (*m/z*)	FA-EA Phosphate (*m/z*)
P-EA NAPE (relative intensity)					P-EA phosphate
1041	7.27e7	283: (18:0)	339: (22:0)	719	378
1027	6.77e7	281: (18:1)	327: (22:6)	717	378
1097	5.50e7	367: (24:0)	311: (20:0)	803	378
1083	5.40e7	335: (22:2)	329: (22:5)	771	378
AL-EA NAPE					AL-EA phosphate
1083	5.40e7	277: (18:3)	365: (24:1)	735	400
1055	4.94e7	359: (24:4)	255: (16:0)	817	400
L-EA NAPE					L-EA phosphate
1027	6.77e7	329: (22:5)	255: (16:0)	789	402
1083	5.40e7	283: (18:0)	357: (24:5)	743	402
1055	4.94e7	307: (20:2)	305: (20:3)	767	402
O-EA NAPE					O-EA phosphate
1027	6.77e7	255: (16:0)	327: (22:6)	717	404
1083	5.40e7	309: (20:1)	329: (22:5)	771	404
1055	4.94e7	281: (18:1)	339: (20:5)	733	404
ST-EA NAPE					ST-EA phosphate
1041	7.27e7	255: (16:0)	339: (22:0)	719	406
1027	6.77e7	253: (16:1)	327: (22:6)	717	406
1097	5.50e7	339: (22:0)	311: (20:0)	803	406
1083	5.40e7	307: (20:2)	329: (22:5)	771	406
A-EA NAPE					A-EA phosphate
1027	6.77e7	305: (20:3)	255: (16:0)	789	426
1083	5.40e7	311: (20:0)	305: (20:3)	795	426
1055	4.94e7	333: (22:3)	255: (16:0)	817	426
DH-EA NAPE					DH-EA phosphate
1027	6.77e7	281: (18:1)	255: (16:0)	789	450
1097	5.50e7	277: (18:3)	329: (22:5)	785	450
1083	5.40e7	227: (14:0)	365: (24:1)	735	450
1055	4.94e7	309: (20:1)	255: (16:0)	817	450

sn-2 lyso NAPE (*m/z*), [NAPE-*sn*-2FA+OH](*m/z*).

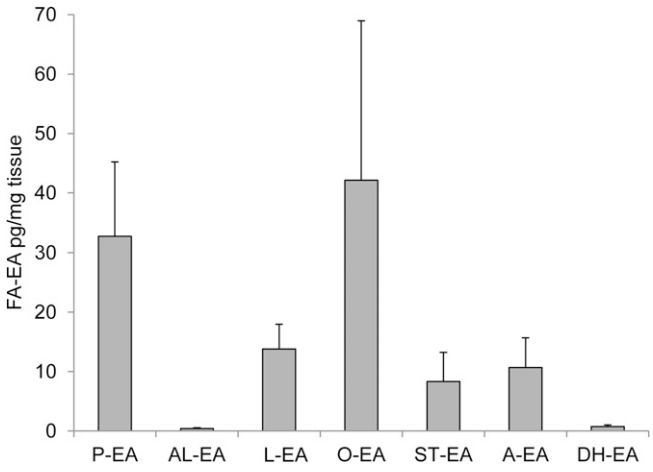

Fig. 7. Anandamide and other FA-EAs detected in rabbit corneal extract. Results expressed as pg/mg tissue ± SD (n = 4 independent experiments). The LC/ESI-MS/MS assay was based on the following MRM transitions: P-EA, *m/z* 300 > 62; AL-EA, *m/z* 322 > 62; L-EA, *m/z* 324 > 62; O-EA, *m/z* 326 > 62; ST-EA, *m/z* 328 > 62; A-EA, *m/z* 348 > 62; and DH-EA, *m/z* 372 > 62. Chromatographic conditions are described in Materials and Methods.

amino ethanol head group) and identified an indomethacin sensitive peak with retention time ~1.2 min. Although these observations suggest the formation of PGI_2-EA, further work using a synthetic standard is needed to confirm and further explore this finding.

The prevalence of PGs $PGF_{2\alpha}$, PGE_2, and PGD_2 supports the identification of prostamides $PGF_{2\alpha}$-EA, PGE_2-EA, and PGD_2-EA and points to the presence of functionally active PGFS, PGES, and PGDS isoforms in the cornea. Although production of the $PGF_{2\alpha}$ was ~4-fold lower than both PGE_2 and PGD_2, prostamide $PGF_{2\alpha}$-EA was identified at relatively higher levels following external addition of A-EA substrate. This could be possibly attributed to the prevalence of prostamide/PGFS synthase in the corneal tissue. This synthase has been reported in mouse eye, although its exact location in the ocular tissues was not reported and the activity was found to be much lower compared with brain or heart tissue (12, 59, 60).

The inactivation of PGE_2 and $PGF_{2\alpha}$ as evidenced by the presence of 13, 14-dihydro 15-keto PGE_2 and 13, 14-dihydro 15-keto $PGF_{2\alpha}$ suggests the presence of functionally active 15-PGDH in the rabbit cornea. This new finding provides valuable information on corneal function, suggesting that this tissue actively controls the production of PGs, and may have implications for the modulation of pain and injury. It also raises the possibility that the low levels of prostamides PGE_2-EA and PGD_2-EA detected in the corneal tissue could be a consequence of their metabolism by 15-PGDH (61). Studies have showed that $PGF_{2\alpha}$-glyceryl ester is a poor substrate for 15-PGDH compared with the free acid, and it is plausible that $PGF_{2\alpha}$-EA may also be less efficiently oxidized (61); this together with the potential prevalence of a prostamide/PGFS synthase in the cornea (59) could contribute to relatively higher levels of $PGF_{2\alpha}$-EA, as reported in the present study.

In conclusion, the novel findings presented herein provide evidence that the pathway for the biosynthesis of PG-EA is operational in the cornea and, as such, constitutes a distinct target for modulating pain perception through use of FAAH and COX-2 inhibitors, in a way that is independent from the classical PG pathway. In addition, the congeners of A-EA were detected and quantified, which provides valuable insight into corneal physiology and those tissues that are anatomically adjacent. Thus, it is possible that corneal FA-EA and their biosynthetic precursors may influence a proximal region, such as the endothelial cells of Schlemm's canal. These studies provide rationale for such future investigations.

The authors thank Waters Ltd. (Manchester, UK) and Andrew Healey (Analytical Centre, University of Bradford) for excellent technical support.

REFERENCES

1. Srinivas, S. P. 2010. Dynamic regulation of barrier integrity of the corneal endothelium. *Optom. Vis. Sci.* **87:** E239–E254.
2. Maddula, S., D. K. Davis, M. K. Burrow, and B. K. Ambati. 2011. Horizons in therapy for corneal angiogenesis. *Ophthalmology.* **118:** 591–599.
3. Cursiefen, C. 2007. Immune privilege and angiogenic privilege of the cornea. *Chem. Immunol. Allergy.* **92:** 50–57.
4. Chen, K. H., W. M. Hsu, C. C. Chiang, and Y. S. Li. 2003. Transforming growth factor-beta2 inhibition of corneal endothelial proliferation mediated by prostaglandin. *Curr. Eye Res.* **26:** 363–370.
5. Daniel, T. O., H. Liu, J. D. Morrow, B. C. Crews, and L. J. Marnett. 1999. Thromboxane A2 is a mediator of cyclooxygenase-2-dependent endothelial migration and angiogenesis. *Cancer Res.* **59:** 4574–4577.
6. Black, A. T., M. K. Gordon, D. E. Heck, M. A. Gallo, D. L. Laskin, and J. D. Laskin. 2011. UVB light regulates expression of antioxidants and inflammatory mediators in human corneal epithelial cells. *Biochem. Pharmacol.* **81:** 873–880.
7. Liclican, E. L., V. Nguyen, A. B. Sullivan, and K. Gronert. 2010. Selective activation of the prostaglandin E2 circuit in chronic injury-induced pathologic angiogenesis. *Invest. Ophthalmol. Vis. Sci.* **51:** 6311–6320.
8. Murata, T., M. I. Lin, K. Aritake, S. Matsumoto, S. Narumiya, H. Ozaki, Y. Urade, M. Hori, and W. C. Sessa. 2008. Role of prostaglandin D2 receptor DP as a suppressor of tumor hyperpermeability and angiogenesis in vivo. *Proc. Natl. Acad. Sci. USA.* **105:** 20009–20014.
9. Woodward, D. F., A. H. Krauss, J. Chen, Y. Liang, C. Li, C. E. Protzman, A. Bogardus, R. Chen, K. M. Kedzie, H. A. Krauss, et al. 2003. Pharmacological characterization of a novel antiglaucoma agent, Bimatoprost (AGN 192024). *J. Pharmacol. Exp. Ther.* **305:** 772–785.
10. Yu, M., D. Ives, and C. S. Ramesha. 1997. Synthesis of prostaglandin E2 ethanolamide from anandamide by cyclooxygenase-2. *J. Biol. Chem.* **272:** 21181–21186.
11. Kozak, K. R., B. C. Crews, J. D. Morrow, L. H. Wang, Y. H. Ma, R. Weinander, P. J. Jakobsson, and L. J. Marnett. 2002. Metabolism of the endocannabinoids, 2-arachidonylglycerol and anandamide, into prostaglandin, thromboxane, and prostacyclin glycerol esters and ethanolamides. *J. Biol. Chem.* **277:** 44877–44885.
12. Koda, N., Y. Tsutsui, H. Niwa, S. Ito, D. F. Woodward, and K. Watanabe. 2004. Synthesis of prostaglandin F ethanolamide by prostaglandin F synthase and identification of Bimatoprost as a potent inhibitor of the enzyme: new enzyme assay method using LC/ESI/MS. *Arch. Biochem. Biophys.* **424:** 128–136.
13. Yang, W., J. Ni, D. F. Woodward, D. D. Tang-Liu, and K. H. Ling. 2005. Enzymatic formation of prostamide F2alpha from anandamide involves a newly identified intermediate metabolite, prostamide H2. *J. Lipid Res.* **46:** 2745–2751.

14. Ueda, N., K. Tsuboi, and T. Uyama. 2013. Metabolism of endocannabinoids and related N-acylethanolamines: canonical and alternative pathways. *FEBS J.* **280:** 1874–1894.
15. Liu, J., L. Wang, J. Harvey-White, B. X. Huang, H. Y. Kim, S. Luquet, R. D. Palmiter, G. Krystal, R. Rai, A. Mahadevan, et al. 2008. Multiple pathways involved in the biosynthesis of anandamide. *Neuropharmacology.* **54:** 1–7.
16. Cravatt, B. F., D. K. Giang, S. P. Mayfield, D. L. Boger, R. A. Lerner, and N. B. Gilula. 1996. Molecular characterization of an enzyme that degrades neuromodulatory fatty-acid amides. *Nature.* **384:** 83–87.
17. Tsuboi, K., N. Takezaki, and N. Ueda. 2007. The N-acylethanolamine-hydrolyzing acid amidase (NAAA). *Chem. Biodivers.* **4:** 1914–1925.
18. Ritter, J. K., C. Li, M. Xia, J. L. Poklis, A. H. Lichtman, R. A. Abdullah, W. L. Dewey, and P. L. Li. 2012. Production and actions of the anandamide metabolite prostamide E2 in the renal medulla. *J. Pharmacol. Exp. Ther.* **342:** 770–779.
19. Patsos, H. A., D. J. Hicks, R. R. Dobson, A. Greenhough, N. Woodman, J. D. Lane, A. C. Williams, and C. Paraskeva. 2005. The endogenous cannabinoid, anandamide, induces cell death in colorectal carcinoma cells: a possible role for cyclooxygenase 2. *Gut.* **54:** 1741–1750.
20. Andrianova, E. L., E. E. Genrikhs, M. Y. Bobrov, A. A. Lizhin, N. M. Gretskaya, L. E. Frumkina, L. G. Khaspekov, and V. V. Bezuglov. 2011. In vitro effects of anandamide and prostamide e2 on normal and transformed nerve cells. *Bull. Exp. Biol. Med.* **151:** 30–32.
21. Gatta, L., F. Piscitelli, C. Giordano, S. Boccella, A. Lichtman, S. Maione, and V. Di Marzo. 2012. Discovery of prostamide F2alpha and its role in inflammatory pain and dorsal horn nociceptive neuron hyperexcitability. *PLoS ONE.* **7:** e31111.
22. Spada, C. S., A. H. Krauss, D. F. Woodward, J. Chen, C. E. Protzman, A. L. Nieves, L. A. Wheeler, D. F. Scott, and G. Sachs. 2005. Bimatoprost and prostaglandin F(2 alpha) selectively stimulate intracellular calcium signaling in different cat iris sphincter cells. *Exp. Eye Res.* **80:** 135–145.
23. Woodward, D. F., A. H. Krauss, J. W. Wang, C. E. Protzman, A. L. Nieves, Y. Liang, Y. Donde, R. M. Burk, K. Landsverk, and C. Struble. 2007. Identification of an antagonist that selectively blocks the activity of prostamides (prostaglandin-ethanolamides) in the feline iris. *Br. J. Pharmacol.* **150:** 342–352.
24. Matias, I., J. Chen, L. De Petrocellis, T. Bisogno, A. Ligresti, F. Fezza, A. H. Krauss, L. Shi, C. E. Protzman, C. Li, et al. 2004. Prostaglandin ethanolamides (prostamides): in vitro pharmacology and metabolism. *J. Pharmacol. Exp. Ther.* **309:** 745–757.
25. Hernangómez, M., L. Mestre, F. G. Correa, F. Loría, M. Mecha, P. M. Iñigo, F. Docagne, R. O. Williams, J. Borrell, and C. Guaza. 2012. CD200–CD200R1 interaction contributes to neuroprotective effects of anandamide on experimentally induced inflammation. *Glia.* **60:** 1437–1450.
26. Russo, R., J. Loverme, G. La Rana, T. R. Compton, J. Parrott, A. Duranti, A. Tontini, M. Mor, G. Tarzia, A. Calignano, et al. 2007. The fatty acid amide hydrolase inhibitor URB597 (cyclohexylcarbamic acid 3′-carbamoylbiphenyl-3-yl ester) reduces neuropathic pain after oral administration in mice. *J. Pharmacol. Exp. Ther.* **322:** 236–242.
27. Pate, D. W., K. Järvinen, A. Urtti, P. Jarho, and T. Järvinen. 1995. Ophthalmic arachidonylethanolamide decreases intraocular pressure in normotensive rabbits. *Curr. Eye Res.* **14:** 791–797.
28. Luchicchi, A., and M. Pistis. 2012. Anandamide and 2-arachidonoylglycerol: pharmacological properties, functional features, and emerging specificities of the two major endocannabinoids. *Mol. Neurobiol.* **46:** 374–392.
29. Coulon, D., L. Faure, M. Salmon, V. Wattelet, and J. J. Bessoule. 2012. Occurrence, biosynthesis and functions of N-acylphosphatidylethanolamines (NAPE): not just precursors of N-acylethanolamines (NAE). *Biochimie.* **94:** 75–85.
30. Wellner, N., T. A. Diep, C. Janfelt, and H. S. Hansen. 2013. N-acylation of phosphatidylethanolamine and its biological functions in mammals. *Biochim. Biophys. Acta.* **1831:** 652–662.
31. Ahn, K., D. S. Johnson, M. Mileni, D. Beidler, J. Z. Long, M. K. McKinney, E. Weerapana, N. Sadagopan, M. Liimatta, S. E. Smith, et al. 2009. Discovery and characterization of a highly selective FAAH inhibitor that reduces inflammatory pain. *Chem. Biol.* **16:** 411–420.
32. Astarita, G., and D. Piomelli. 2009. Lipidomic analysis of endocannabinoid metabolism in biological samples. *J. Chromatogr. B Analyt. Technol. Biomed. Life Sci.* **877:** 2755–2767.
33. Kingsley, P. J., and L. J. Marnett. 2009. Analysis of endocannabinoids, their congeners and COX-2 metabolites. *J. Chromatogr. B Analyt. Technol. Biomed. Life Sci.* **877:** 2746–2754.
34. Masoodi, M., and A. Nicolaou. 2006. Lipidomic analysis of twenty-seven prostanoids and isoprostanes by liquid chromatography/electrospray tandem mass spectrometry. *Rapid Commun. Mass Spectrom.* **20:** 3023–3029.
35. Masoodi, M., A. A. Mir, N. A. Petasis, C. N. Serhan, and A. Nicolaou. 2008. Simultaneous lipidomic analysis of three families of bioactive lipid mediators leukotrienes, resolvins, protectins and related hydroxy-fatty acids by liquid chromatography/electrospray ionisation tandem mass spectrometry. Rapid *C*ommun. *M*ass *S*pectrom. **22:** 75–83.
36. Astarita, G., F. Ahmed, and D. Piomelli. 2008. Identification of biosynthetic precursors for the endocannabinoid anandamide in the rat brain. *J. Lipid Res.* **49:** 48–57.
37. Weber, A., J. Ni, K. H. Ling, A. Acheampong, D. D. Tang-Liu, R. Burk, B. F. Cravatt, and D. Woodward. 2004. Formation of prostamides from anandamide in FAAH knockout mice analyzed by HPLC with tandem mass spectrometry. *J. Lipid Res.* **45:** 757–763.
38. Tai, H. H. 2011. Prostaglandin catabolic enzymes as tumor suppressors. *Cancer Metastasis Rev.* **30:** 409–417.
39. Beermann, C., M. Mobius, N. Winterling, J. J. Schmitt, and G. Boehm. 2005. sn-position determination of phospholipid-linked fatty acids derived from erythrocytes by liquid chromatography electrospray ionization ion-trap mass spectrometry. *Lipids.* **40:** 211–218.
40. Reddy, P. V., V. Natarajan, P. C. Schmid, and H. H. Schmid. 1983. N-Acylation of dog heart ethanolamine phospholipids by transacylase activity. *Biochim. Biophys. Acta.* **750:** 472–480.
41. Bisogno, T., I. Delton-Vandenbroucke, A. Milone, M. Lagarde, and V. Di Marzo. 1999. Biosynthesis and inactivation of N-arachidonoylethanolamine (anandamide) and N-docosahexaenoylethanolamine in bovine retina. *Arch. Biochem. Biophys.* **370:** 300–307.
42. Stinson, A. M., R. D. Wiegand, and R. E. Anderson. 1991. Fatty acid and molecular species compositions of phospholipids and diacylglycerols from rat retinal membranes. *Exp. Eye Res.* **52:** 213–218.
43. Nakanishi, H., Y. Iida, T. Shimizu, and R. Taguchi. 2010. Separation and quantification of sn-1 and sn-2 fatty acid positional isomers in phosphatidylcholine by RPLC-ESIMS/MS. *J. Biochem.* **147:** 245–256.
44. Garcia-Ovejero, D., A. Arevalo-Martin, S. Petrosino, F. Docagne, C. Hagen, T. Bisogno, M. Watanabe, C. Guaza, V. Di Marzo, and E. Molina-Holgado. 2009. The endocannabinoid system is modulated in response to spinal cord injury in rats. *Neurobiol. Dis.* **33:** 57–71.
45. Rani Sagar, D., J. J. Burston, S. G. Woodhams, and V. Chapman. 2012. Dynamic changes to the endocannabinoid system in models of chronic pain. *Philos. Trans. R. Soc. Lond. B Biol. Sci.* **367:** 3300–3311.
46. Correa, F., M. Hernangomez, L. Mestre, F. Loria, A. Spagnolo, F. Docagne, V. Di Marzo, and C. Guaza. 2010. Anandamide enhances IL-10 production in activated microglia by targeting CB(2) receptors: roles of ERK1/2, JNK, and NF-kappaB. *Glia.* **58:** 135–147.
47. Bereiter, D. A., D. F. Bereiter, and H. Hirata. 2002. Topical cannabinoid agonist, WIN55,212–2, reduces cornea-evoked trigeminal brainstem activity in the rat. *Pain.* **99:** 547–556.
48. Yang, H., Z. Wang, J. E. Capo-Aponte, F. Zhang, Z. Pan, and P. S. Reinach. 2010. Epidermal growth factor receptor transactivation by the cannabinoid receptor (CB1) and transient receptor potential vanilloid 1 (TRPV1) induces differential responses in corneal epithelial cells. *Exp. Eye Res.* **91:** 462–471.
49. Pisanti, S., P. Picardi, L. Prota, M. C. Proto, C. Laezza, P. G. McGuire, L. Morbidelli, P. Gazzerro, M. Ziche, A. Das, et al. 2011. Genetic and pharmacologic inactivation of cannabinoid CB1 receptor inhibits angiogenesis. *Blood.* **117:** 5541–5550.
50. Chen, J., I. Matias, T. Dinh, T. Lu, S. Venezia, A. Nieves, D. F. Woodward, and V. Di Marzo. 2005. Finding of endocannabinoids in human eye tissues: implications for glaucoma. *Biochem. Biophys. Res. Commun.* **330:** 1062–1067.
51. Petrosino, S., T. Iuvone, and V. Di Marzo. 2010. N-palmitoylethanolamine: biochemistry and new therapeutic opportunities. *Biochimie.* **92:** 724–727.
52. Esposito, E., and S. Cuzzocrea. 2013. Palmitoylethanolamide is a new possible pharmacological treatment for the inflammation associated with trauma. *Mini Rev. Med. Chem.* **13:** 237–255.
53. Thabuis, C., D. Tissot-Favre, J. B. Bezelgues, J. C. Martin, C. Cruz-Hernandez, F. Dionisi, and F. Destaillats. 2008. Biological

functions and metabolism of oleoylethanolamide. *Lipids.* **43:** 887–894.
54. Bradbury, J. 2011. Docosahexaenoic acid (DHA): an ancient nutrient for the modern human brain. *Nutrients.* **3:** 529–554.
55. Fowler, C. J. 2012. NSAIDs: eNdocannabinoid stimulating anti-inflammatory drugs? *Trends Pharmacol. Sci.* **33:** 468–473.
56. Hermanson, D. J., N. D. Hartley, J. Gamble-George, N. Brown, B. C. Shonesy, P. J. Kingsley, R. J. Colbran, J. Reese, L. J. Marnett, and S. Patel. 2013. Substrate-selective COX-2 inhibition decreases anxiety via endocannabinoid activation. *Nat. Neurosci.* **16:** 1291–1298.
57. Yang, H. Y., F. Karoum, C. Felder, H. Badger, T. C. Wang, and S. P. Markey. 1999. GC/MS analysis of anandamide and quantification of N-arachidonoylphosphatidylethanolamides in various brain regions, spinal cord, testis, and spleen of the rat. *J. Neurochem.* **72:** 1959–1968.
58. Deutsch, D. G., M. S. Goligorsky, P. C. Schmid, R. J. Krebsbach, H. H. Schmid, S. K. Das, S. K. Dey, G. Arreaza, C. Thorup, G. Stefano, et al. 1997. Production and physiological actions of anandamide in the vasculature of the rat kidney. *J. Clin. Invest.* **100:** 1538–1546.
59. Moriuchi, H., N. Koda, E. Okuda-Ashitaka, H. Daiyasu, K. Ogasawara, H. Toh, S. Ito, D. F. Woodward, and K. Watanabe. 2008. Molecular characterization of a novel type of prostamide/prostaglandin F synthase, belonging to the thioredoxin-like superfamily. *J. Biol. Chem.* **283:** 792–801.
60. Urade, Y., K. Watanabe, and O. Hayaishi. 1995. Prostaglandin D, E, and F synthases. *J. Lipid Mediat. Cell Signal.* **12:** 257–273.
61. Kozak, K. R., B. C. Crews, J. L. Ray, H. H. Tai, J. D. Morrow, and L. J. Marnett. 2001. Metabolism of prostaglandin glycerol esters and prostaglandin ethanolamides in vitro and in vivo. *J. Biol. Chem.* **276:** 36993–36998.